Turkish Journal of Electrical Engineering & Computer Sciences

http://journals.tubitak.gov.tr/elektrik/

Research Article

Turk J Elec Eng & Comp Sci
(2017) 25: 3738 – 3751

doi:10.3906/elk-1606-160

Feedback delay compensation of a visual servoing system using a piecewise continuous and current estimator-based observer

Abdeldafia MOHAMMED[1], Haoping WANG[2,*], Yang TIAN[1]
[1]School of Automation, Nanjing University of Science and Technology, Nanjing, P.R. China
[2]Sino-French International Joint Laboratory of Automatic and Signal Processing (LaFAS), School of Automation, Nanjing University of Science and Technology, Nanjing, P.R. China

Received: 11.06.2016 • **Accepted/Published Online:** 30.05.2017 • **Final Version:** 05.10.2017

Abstract: In this paper, a piecewise continuous current estimator-based observer is proposed to estimate a plant's states using sampled and delayed measurements. The advantage of the proposed technique is simple in terms of analysis and design. Moreover, the proposed observer can compensate the time delay when the delay equals the sampling period. Comprehensive stability analysis of the designed observer is performed. In addition, to assess the efficiency and effectiveness of the proposed observer, a numerical comparative study with a Kalman filter-based observer is established and the simulation results are demonstrated.

Key words: Piecewise continuous systems, sampled and delayed measurements, piecewise continuous current estimator

1. Introduction

A visual servoing system (VSS) is a kind of system that uses vision data as a feedback signal to control an object's motion [1]. It comprises a controller, robots, and a vision system. During the last two decades, VSSs have been broadly used to increase the accuracy and the flexibility of robotic systems [2,3].

VSSs can be utilized in many applications such as building automation (surveillance), games (soccer robots), and industrial zones (cooperative). Nonetheless, VSSs are facing a great challenge due to the use of visual information in the feedback channel. The time delay in the feedback channel occurs by image acquisition, image processing, and information transmission [4,5]. The time delay is well known to be a resource of instability and degrades the system's performance.

Generally, the sensors that are based on vision have a larger sampling period than the other types of sensors due to the restricted constraints the vision sensors have in communication and snapshot speed [6–8].

In the literature, various control design methods were presented to handle systems with time delay. In [9–11] researchers studied the delay problem by utilizing standard analysis methods from robust control, and good control performances were observed. The analysis of the problem was investigated under the assumption that the time delay in the feedback channel is less than one sampling period. However, the control performance will be affected by increasing the sampling period, and it might be ineffective, particularly in high-speed dynamical systems.

On the other hand, designs of nondelay state observers for systems with the above-mentioned problems have been proposed in several approaches such as a continuous approach, which designs a continuous time

*Correspondence: hp.wang@njust.edu.cn

observer based on the continuous time plant model. The weakness of this approach is the neglect of the sampling of the output and the closed-loop system stability is assured only under a small sampling period [12–14]. Based on the hybrid systems approach a piecewise continuous observer was proposed in [15,16]. The benefit of this approach is that it takes into account sampling and delay and is simpler compared with other approaches. Based on the continuous-time Lyapunov–Krasovskii approach, the Lyapunov–Krasovskii observer was proposed in [17]. The advantage of this approach is the robust stability in the case of uncertainties in the system parameters and sampling period. The disadvantage of this approach is an imperative solution of complex linear matrix inequalities.

This work proposes a different approach to the observer design based on a piecewise continuous system and current estimator, and the observer gain is selected based on a linear matrix inequality (LMI) to guarantee the stability of the dynamics error. In this approach, the solution of complex linear matrix inequalities is not compulsory.

This paper considers the delay in the feedback channel from sampled and delayed measurement. The goal is to design the observer based on the piecewise continuous system and current estimator to estimate the nondelay continuous state.

The main contributions of this work are as follows: 1) it compensates the time delay in a feedback channel with a simpler estimator structural design than the aforesaid approaches; 2) it estimates the nondelayed continuous state from the sampled and delayed measurement; 3) with respect to the existing results, accuracy and fast computation are achieved when the time delay is equal to the sampling period. In order to demonstrate the performance superiority of the proposed observer, a comparison with the Kalman filter-based approach proposed in [13,14] has been performed.

The rest of this paper is organized as follows: in Section 2, the problem formulation and introduction to the plant are given. Section 3 presents the piecewise continuous system and observer design. In Section 4, the observer dynamics and stability are presented. In Section 5, an overview of the Kalman filter-based observer is provided. The numerical simulation example is demonstrated in Section 6. Finally, concluding remarks and recommendations for future work are given in Section 7.

2. Problem formulation

The VSS structure considered in this paper is shown in Figure 1. In our study, the only available plant information is obtained through the digital sensor (camera), which introduces time delay as a consequence of image acquisition, image processing, and visual information transmission. The digital sensor determines the object position to be manipulated and delivers it in a sampled and delayed form (see Figure 2).

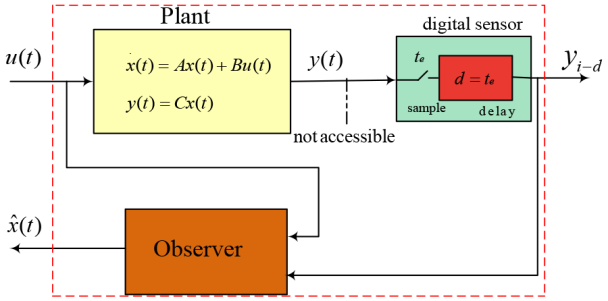

Figure 1. The VSS structure considered.

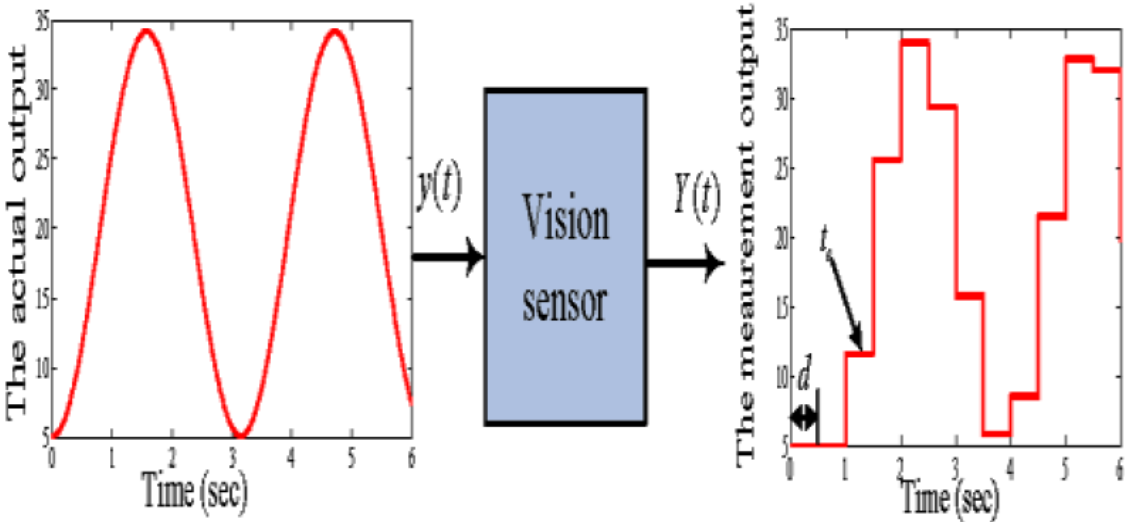

Figure 2. The real output and its measurement.

The system dynamics is linear time-invariant (LTI) and it can be described as follows:

$$\begin{cases} \dot{x}(t) = Ax(t) + Bu(t) \\ y(t) = Cx(t) \end{cases}, \tag{1}$$

where $u(t) \in \Re^r$ is the control input and $x(t) \in \Re^n$ is the state, $y(t) \in \Re^m$ is the output of the plant, and $A \in \Re^{n\times n}, B \in \Re^{n\times r}, C \in \Re^{m\times n}$ are constant matrices. It is assumed that the system in Eq. (1) is observable.

Digital sensor information can be specified by:

$$Y(t) = y^*(t-d), \tag{2}$$

where $Y(t)$ is the digital sensor output and represents the visual information of the object position, which is used to estimate the position and velocity of the moving object, and $*$ represents sampling with the known and constant period. d is the time delay that represents the time requirement for image processing and data transmitting and it can be expressed as $d = t_e$, which means that the measures sampled at t_i are available for the observer before the next measures at t_{i+1}, where t_e is the sampling period of the digital sensor.

For simplification, the notation y_{i-d} will be used to represent the sampled and delayed measurement. In this work, t_e is assumed to be known and constant.

As shown in Figure 1, the control design is not considered in our study. The main issue is the time delay between the sensor and controller, which is introduced as a consequence of image acquisition, image processing, and data transmitting. The design of a state observer is a very important issue in estimating the system's continuous nondelayed state $x(t)$ from the sampled and delayed measurement $Y(t)$.

3. Observer design

To deal with a system whose state is not accessible, an observer is proposed to estimate the states. The proposed observer is constructed from two linear piecewise continuous systems and current estimator as shown in Figure 3.

The piecewise continuous system (PCS) is characterized by controlled impulses and autonomous switching [18]. The PCS is a hybrid system that represents a two-time domain, discrete and continuous time. The

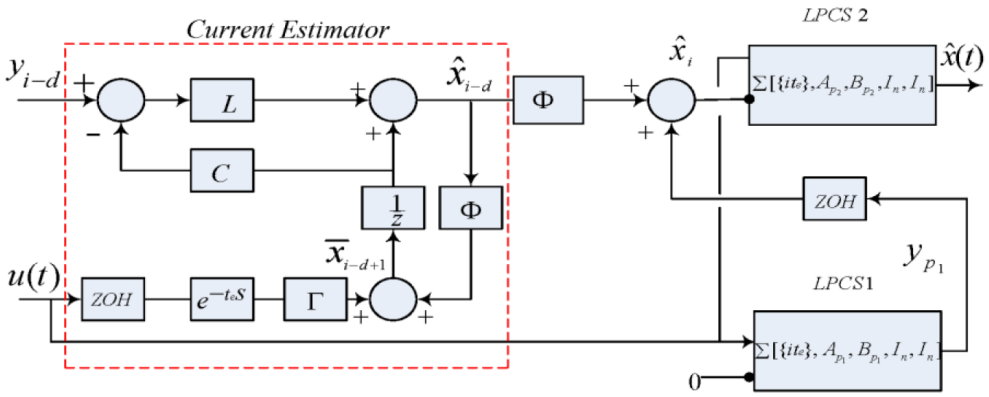

Figure 3. Piecewise continuous current estimator based observer.

discrete time input is defined by S, where $S = \{t_i, i = 0, 1, 2, ..., \}$, and the continuous time input is defined by $\mathrm{T}_t = \{\Im - S\}$, where $\Im = \{t \in [0, \infty]\}$. Both inputs determine the dynamic of the PCS. At each switching instant, the plant is controlled by a switching input, and between two switching instants it is controlled by a continuous input. Two successive switching instants t_i and t_{i+1} set the boundaries in an interval denoted $\mathrm{T}_i = \{\mathrm{T}_t \,|\forall_t \in]t_i, t_{i+1}[\,\}$.

The linear PCS at $t_i = it_e$ can be described as:

$$x_p(it_e^+) = B_d v_p(it_e) \qquad \forall i \in S, \tag{3a}$$

$$\dot{x}_p(t) = A_p x_p(t) + B_p u_p(t) \qquad \forall t \in \mathrm{T}_t, \tag{3b}$$

$$y_p(t) = C_p x_p(t) \qquad \forall t \in \Im, \tag{3c}$$

where $v_p(t) \in \Re^s, u_p(t) \in \Re^r$ are the switching and continuous inputs, respectively; $x_p(t) \in \Re^n$ is the system state; $y_p(t) \in \Re^m$ is the system output; and $A_p \in \Re^{n\times n} B_p \in \Re^{n\times r}, B_d \in \Re^{n\times s}, C_p \in \Re^{m\times n}$ are constant matrices. Eq. (3a) describes the PCS in the discrete time domain at every time instant, Eq. (3b) describes the dynamic state in the continuous time domain, and Eq. (3c) represents the output of the PCS.

The PCS is denoted as $\sum[\{it_e\}, A_p, B_p, B_d, C_p]$. The PCS is represented symbolically as inputs and output as shown in Figure 4, where the input $v_p(t)$ is denoted by the point symbol and the continuous input $u_p(t)$ is denoted by the usual symbol.

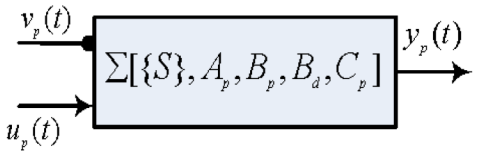

Figure 4. PCS symbolic representation.

The description of Eq. (3b) in time interval $\mathrm{T}_i = \{\mathrm{T}_t \,|\forall t \in]it_e, (i+1)t_e\,\}$ can be given as [18]:

$$x_p(t) = \exp(A_p(t - it_e)x_p(it_e^+) + \int_{it_e}^{t} \exp A_p(t-\tau)B_p u_p(\tau)d\tau \qquad \forall t \in \mathrm{T}_i. \tag{4}$$

Substituting Eq. (3a) into Eq. (4), one can get:

$$x_p(t) = \exp(A_p(t - it_e)B_d v_p(it_e) + \int_{it_e}^{t} \exp A_p(t-\tau)B_p u_p(\tau)d\tau \qquad \forall t \in \mathrm{T}_i. \tag{5}$$

The left limit $x_p(it_e^-)$ of $x_p(t)$ at $t = it_e$ can be acquired from Eq. (5) for the interval t_{i-1}, t_i as follows:

$$x_p(it_e^-) = \exp(A_p t_e)B_d v((i-1)t_e) + \int_{(i-1)t_e}^{it_e} \exp A_p(it_e - \tau)B_p u_p(\tau)d\tau \qquad \forall t \in \mathrm{T}i. \tag{6}$$

Hence, Eqs. (5) and (6) demonstrate that $x(it_e^-) \neq x(it_e^+)$. Figure 5 shows the PCS response.

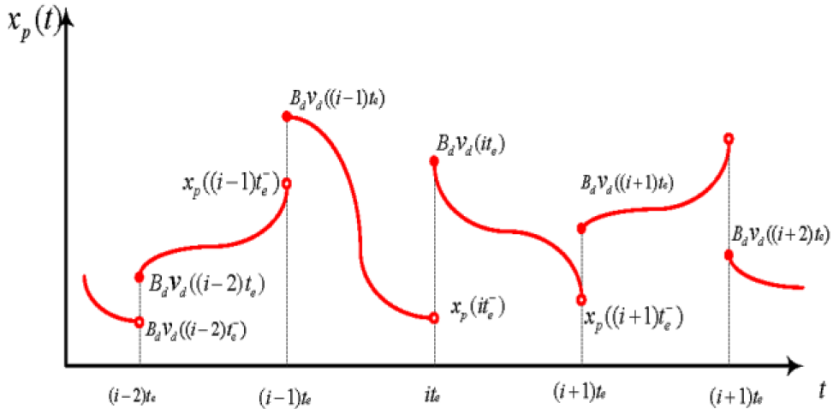

Figure 5. Piecewise continuous system response.

The design procedures of the proposed observer can be described as follows:

First, we discretize the LTI system, i.e. Eq. (1), with sampling period t_e. The discrete model with sampling time is given by:

$$\begin{cases} x_i = \Phi x_{i-1} + \Gamma u_{i-1} \\ y_i = C x_i \end{cases}, \tag{7}$$

where Φ, Γ, and C are constant matrices of appropriate dimensions.

The sampled and delayed state x_{i-d} of Eq. (2) is estimated from the current estimator based on the most recent measurement, y_{i-d}. The current estimator was made by modifying the predictor observer to provide the current estimated state based on the most recent measurement. The current estimator is described by:

$$\bar{x}_{i-d} = \Phi \hat{x}_{i-d-1} + \Gamma u_{i-d-1}, \tag{8a}$$

$$\hat{x}_{i-d} = \bar{x}_{i-d} + L(y_{i-d} - C\bar{x}_{i-d}), \tag{8b}$$

where $\bar{x}_{i-d}$ is the estimated state of x_{i-d} based on the prediction from the previous time step, $\hat{x}_{i-d}$ is the estimated state of the sampled and delayed state x_{i-d}, and L is the observer gain, which can be calculated by any conventional approach of the observer based on the pole placement or optimal state estimation. In this work, the observer gain is determined by LMI and it will be presented in next section.

Second, from linear piecewise continuous system 1 (LPCS1) with $\sum[\{it_e\}, A_{p_1}, B_{p_1}, I_n, I_n]$ and inputs $v_{p_1}(t) = 0$, $u_{p_1}(t) = u(t)$, and constant matrices $A_{p_1} = A, B_{p_1} = B, C_{p_1} = C$, one gets:

$$y_{p_1}(t) = \int_{(i-1)t_e}^{t} \exp A(t-\tau)Bu(\tau)d\tau. \tag{9}$$

Discretizing the output $y_{p_1}(t)$ with sampling period t_e, one obtains:

$$y_{p_1}(it_e) = \int_{(i-1)t_e}^{it_e} \exp A(it_e-\tau)Bu(\tau)d\tau. \tag{10}$$

Then the estimated state without delay $\hat{x}_i$ can be estimated as follows:

$$\hat{x}_i = \Phi\hat{x}_{i-d} + y_{p_1}(it_e) = \Phi\hat{x}_{i-d} + \int_{(i-1)t_e}^{it_e} \exp A(it_e-\tau)Bu(\tau)d\tau. \tag{11}$$

Finally, from linear piecewise continuous system 2 (LPCS2) as $\sum[\{it_e\}, A_{p_2}, B_{p_2}, I_n, I_n]$ with input $u_{p_2}(t) = u(t), v_{p_2}(t) = \hat{x}_i$, and constant matrices $A_{p_1} = A$, $B_{p_2} = B$, $C_{p_2} = C$,

the estimated continuous time state $\hat{x}(t)$ is obtained from the output of LPCS2 as:

$$\hat{x}(t) = e^{A(t-t_i)}\hat{x}_i + \int_{t_i}^{t} \exp A(t-\tau)Bu(\tau)d\tau. \tag{12}$$

4. Stability analysis

To show the observer stability, the estimation error can be described as follows:

$$e(t) = x(t) - \hat{x}(t). \tag{13}$$

The proposed observer is asymptotically stable if and only if the estimation error is asymptotically stable, i.e. $\lim_{t\to\infty} e(t) \to 0$.

For simplified notation, $i - d = m$ and thus $\hat{x}_{i-d} = \hat{x}_m$ and $\bar{x}_{i-d} = \bar{x}_m$.

Considering Eqs. (11) and (12), the estimated state can be written as:

$$\hat{x}(t) = e^{A(t-t_i)}[e^{At_e}\hat{x}_m + y_{p_1}(it_e)] + \int_{t_i}^{t} \exp A(t-\tau)Bu(\tau)d\tau, \tag{14}$$

$$\hat{x}(t) = e^{A(t-t_m)}\hat{x}_m + e^{A(t-t_i)}y_{p_1}(it_e) + \int_{t_i}^{t} \exp A(t-\tau)Bu(\tau)d\tau, \tag{15}$$

with $t_m = t_{i-d}$.

Similarly, the real-time system state can be equally denoted as:

$$x(t) = e^{A(t-t_m)}x_m + e^{A(t-t_i)}y_{p_1}(it_e) + \int_{t_i}^{t} \exp A(t-\tau)Bu(\tau)d\tau. \tag{16}$$

From Eqs. (15) and (16), the error $e(t)$ can be defined as:

$$e(t) = e^{A(t-t_m)}e_m, \tag{17}$$

where $e_m = x_m - \hat{x}_m$.

State x_m can be obtained from Eq. (7) as follows:

$$x_m = \Phi x_{m-1} + \Gamma u_{m-1}. \tag{18}$$

State $\hat{x}_m$ can be obtained from Eqs. (8a) and (8b) as:

$$\hat{x}_m = \Phi \hat{x}_{m-1} + \Gamma u_{m-1} + L[y_m - C\bar{x}_m]. \tag{19}$$

From Eqs. (18) and (19) the dynamic error is:

$$e_m = \Phi e_{m-1} - LC\bar{e}_m, \tag{20}$$

with $e_{m-1} = x_{m-1} - \hat{x}_{m-1}$.

The dynamic error of previous time step $\bar{e}_m$ can be defined as:

$$\bar{e}_m = x_m - \bar{x}_m = \Phi x_{m-1} + \Gamma u_{m-1} - \Phi \hat{x}_{m-1} - \Gamma u_{m-1} = \Phi[x_{m-1} - \hat{x}_{m-1}],$$

$$\bar{e}_m = \Phi e_{m-1}. \tag{21}$$

Substituting Eq. (20) into Eq. (21), one has:

$$e_m = \Phi e_{m-1} - LC\Phi e_{m-1} = [I - LC]\Phi e_{m-1}. \tag{22}$$

The observer gain L can be chosen using the following theorem.

Theorem 1 *Consider that the pairs (Φ, C) of the discrete model described in Eq. (7) are observable; if there exist a symmetric positive definite matrix $P \in \Re^{n\times n}$ and matrix L satisfying the algebraic Lyapunov inequality*

$$\begin{bmatrix} -P & (P\Phi - YC\Phi)^T \\ P\Phi - YC\Phi & -P \end{bmatrix} < 0, \tag{23}$$

the observer gain can be calculated by $L = P^{-1}Y$. Therefore, the current estimator described in Eq. (8b) is stable and its estimation error asymptotically converges to zero.

Proof In order to verify that the resulting estimator is stable, consider the following

Lyapunov function:

$$V_m = (e_m)^T P e_m.$$

Taking into account the observation error in Eq. (22), the estimation error e_m converges asymptotically to zero if the following condition is satisfied:

$$\Delta V_m = e_{m+1} - e_m < 0, \qquad \forall e_m \in \Re^n.$$

Therefore:

$$\Delta V_m = (e_{m+1})^T P e_{m+1} - (e_m)^T P e_m < 0$$

$$= ([\Phi - LC\Phi]e_m)^T P([\Phi - LC\Phi]e_m) - (e_m)^T P e_m < 0$$

$$= (e_m)^T \left((\Phi - LC\Phi)^T P((\Phi - LC\Phi)e_m) - P e_m\right) < 0$$

$$= (e_m)^T \left((\Phi - LC\Phi)^T P(\Phi - LC\Phi) - P\right) e_m < 0,$$

$$\Delta Vm = (\Phi - LC\Phi)^T P(\Phi - LC\Phi) - P < 0$$

$$\Leftrightarrow (\Phi - LC\Phi)^T P(\Phi - LC\Phi) - P < 0. \tag{24}$$

Consistent with the Schur complement in [19], Eq. (23) is equivalent to Eq. (24) and $Y = PL$. □

Remark 1 Theorem 1 provides a necessary and sufficient condition for the asymptotic stability of the estimation error, i.e. the observer design L can guarantee fast convergence of $\hat{x}_{m-1}$ towards x_{m-1}. Therefore, e_{m-1} converges quickly to zero and hence e_m. In consequence, the estimation error $e(t)$ converges asymptotically to zero. Furthermore, it ensures the robust performance with respect to the uncertainties of the plant. By using the MATLAB toolbox, a feasible solution of Eq. (23) can be easily founded.

5. Overview of Kalman filter-based observer (KFBO)

The proposed PCCEBO is compared with the KFBO, which was proposed in [13,14], to demonstrate the PCCEBO's performance. The KFBO was proposed for estimating the noisy and delayed measurement.

The dynamic equation can be described as follows:

$$\dot{\hat{x}}(t-d) = [A - KC]\hat{x}(t-d) + Bu(t-d) + Ky(t-d), \tag{25}$$

where d is the time delay. K is the observer gain and it can be calculated by:

$$K = P_r C^T R, \tag{26}$$

and P_r is the solution of the Riccati equation that is described as follows:

$$AP_r + P_r A^T - P_r C^T R^{-1} C P_r + Q = 0, \tag{27}$$

where Q and R are positive-definite covariance matrices for the noisy and delayed measurement. To remove the delay effect from the estimated states, a function g is defined as:

$$\dot{g}(t) = Ag(t) + Bu(t). \tag{28}$$

Finally, the nondelayed state estimate can be found as:

$$\hat{x}(t) = g(t) + e^{Ad}[\hat{x}(t-d) - g(t-d)]. \tag{29}$$

Remark 2 It worth mentioning that the KFBO is neglecting the sampling period in the observer design. Moreover, the observer gain K depends on the covariance matrix Q and R, the covariance matrices are tuned by trial and error. Thus, the performance of the KFBO has a problem with tradeoff between accuracy and fast computation. In practice, it is not easy to determine the exact covariance matrix.

6. Numerical example

In this section, the effectiveness of the proposed observer is illustrated via comparison with the KFBO that was introduced in Section 5. The comparison has been done in Simulink for the mobile cart visual servoing system as follows:

$$\dot{x}(t) = \begin{bmatrix} 0 & 1 \\ 0 & -122 \end{bmatrix} x(t) + \begin{bmatrix} 0 \\ 355 \end{bmatrix} u(t), \qquad y(t) = \begin{bmatrix} 1 & 0 \end{bmatrix} x(t), \tag{30}$$

where $x(t) = \begin{bmatrix} x_1(t) & x_2(t) \end{bmatrix}^T$ is the system state, which consists of the mobile cart position $x_1(t)$ and velocity $x_2(t)$.

Digital sensor information is described as:

$$Y(t) = y^*(t - 0.2).$$

The time delay is chosen as $d = 0.2$ s, which matches the time needed for image acquisition, processing, and transmitting the information ($t_e = 200$ ms).

The observers have been evaluated in the case of an open-loop test, i.e. the controller is not considered. The control input $u(t)$ is assumed to be a saw-tooth signal with amplitude 10 and frequency 2 rad/s, as shown in Figure 6.

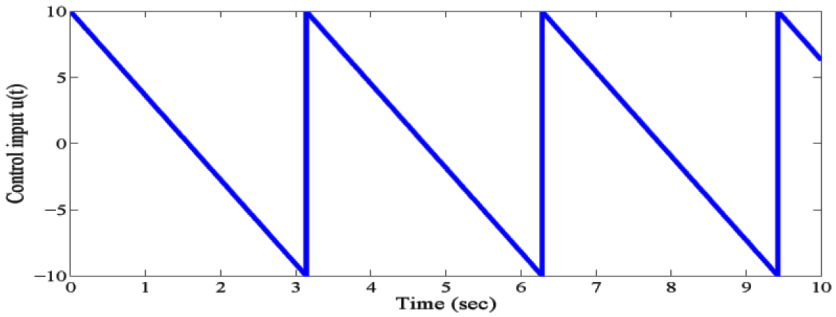

Figure 6. Control input $u(t)$.

The initial conditions for the LTI system and the observer are $x(0) = \begin{bmatrix} 5 & 10 \end{bmatrix}^T, \hat{x}(0) = \begin{bmatrix} 0 & 0 \end{bmatrix}^T$, respectively. The standard routines of the MATLAB LMI control toolbox are used to calculate observer gain L and P in Eq. (23) as follows:

$$P = \begin{bmatrix} 4.9499 & 0.0000 \\ 0.0000 & 4.9499 \end{bmatrix}, Y = \begin{bmatrix} 4.9499 \\ 0.0000 \end{bmatrix}, L = \begin{bmatrix} 1.0000 & 0.0000 \end{bmatrix}^T.$$

On the other hand, to get the gain of the KFBO, Q and R have been chosen as follows: $Q = \begin{bmatrix} 0.001 & 0 \\ 0 & 0.001 \end{bmatrix}, R = 0.004$.

From Eqs. (26) and (27) we can easily obtain the following: $P_r = \begin{bmatrix} 0.0082 & 0.0083 \\ 0.0083 & 1.0329 \end{bmatrix}, K = \begin{bmatrix} 2.0405 & 2.0818 \end{bmatrix}^T$.

The comparison is carried out with and without the existence of measurement noise, as well as in the case of variable system parameters and the case of sampling period equal to 1 s, as presented in the following subsections.

6.1. State estimation without measurement noises

The simulation results of state estimation without measurement noise are shown in Figure 7. Figure 7a illustrates the state of the plant's $x(t)$ state estimated $\hat{x}(t)$ and sampled and delayed measurements y_{i-d}. Figure 7b shows the estimation errors without measurement noise.

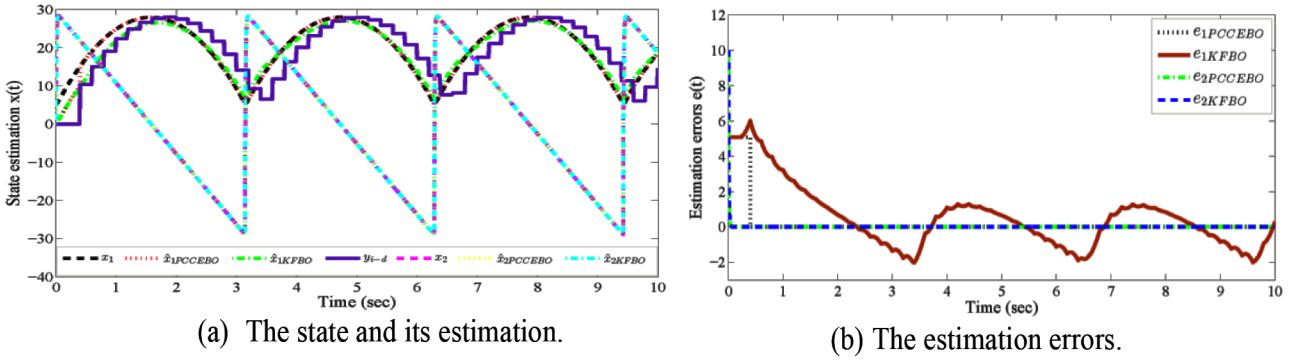

(a) The state and its estimation. (b) The estimation errors.

Figure 7. State estimation without measurement noise: a) the state and its estimation; b) the estimation errors.

The simulation results show that the estimations of PCCEBO convergence are faster than the estimations for the KFBO. Once the convergence is attained, the PCCEBO estimations present better tracking than the KFBO estimations even if the changing of the real state is very fast. Furthermore, the estimation error of the proposed observer is smaller than that of the KFBO. The estimation errors of the PCCEBO are approximately zero after only two sampling periods; obviously in contrast, the estimation error of the KFBO is not converging to zero at this time. One can summarize that the proposed PCCEBO exhibits better performance than the KFBO.

6.2. State estimation with measurement noises

In order to test the robustness of the proposed observer against measurement noise, Gaussian noise with zero mean power has been realized. The measurement noise is added to the digital sensor; therefore, Eq. (2) can be written as follows:

$$Y(t) = y^*(t-d) + v(t), \tag{31}$$

where $v(t)$ is the stochastic measurement noise.

First, the measurement noise is realized with covariance R, which is chosen to make the performance of the KFBO acceptable, but the measurement noise is very small and it is not enough to assess the observer's performance. Therefore, the assessment has been done for covariance $R = 1$ and time delay $d = 0.6$ s. The obtained results are shown in Figure 8. Another type of measurement noise that is realized is the white noise measurement with noise power 0.07, and the corresponding results are shown in Figure 9.

Remark 3 One can see that the KFBO performance is affected with the increasing of covariance R, and it shows a slow response, which implies that the convergence of the estimation errors is attained after a long time,

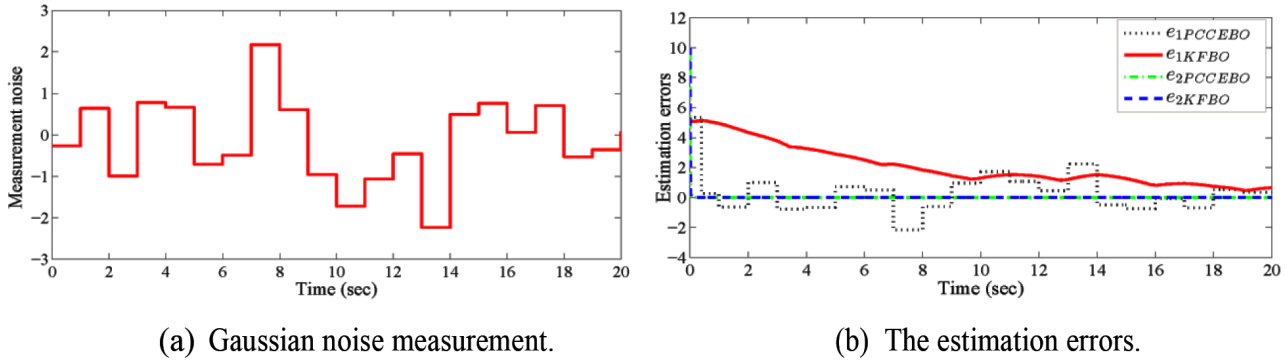

(a) Gaussian noise measurement. (b) The estimation errors.

Figure 8. Observers' performance with Gaussian noise measurement: a) Gaussian noise measurement; b) the estimation errors.

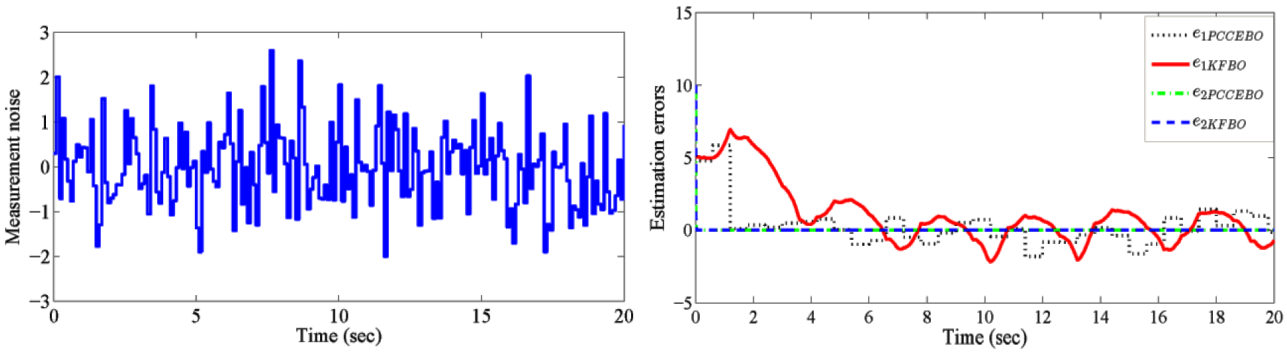

(a) White noise measurement. (b) The estimation errors.

Figure 9. Observers' performance with white noise measurement: a) white noise measurement; b) the estimation errors.

as presented in Figure 8. Nonetheless, it is known that the KFBO is very effective for large measurement noise and in particular Gaussian noise, while the PCCEBO is effective for bounded measurement noise. The proposed PCCEBO under the considered measurement noise presents better responses and faster convergence, and the estimation errors of the PCCEBO are smaller than the estimation errors of the KFBO.

6.3. State estimation in case of variable system parameters

In this part, all parameters are set to the same values of the parameters in Subsection 6.1. In order to show the sensitivity of the proposed observer to parameter variations, it is assumed that over longer periods, the parameters of the system of Eq. (1) have slow variations as follows:

$$A = \begin{bmatrix} 0 & 1 \\ 0 & A_{22} \end{bmatrix}, B = \begin{bmatrix} 0 \\ B_{21} \end{bmatrix} \text{ where } A_{22} = -120 - (4\sin 10t + 20\cos t \sin t), \text{ and } B_{21} = 355 + 20\sin 2t \cos 2t.$$

The corresponding results are shown in Figure 10. The results show that the PCCEBO is less sensitive to the considered parameters variations.

6.4. State estimation when the sampling period is not small

In this case, numerical simulations have been conducted for $d = t_e = 1$ s with the following parameters:

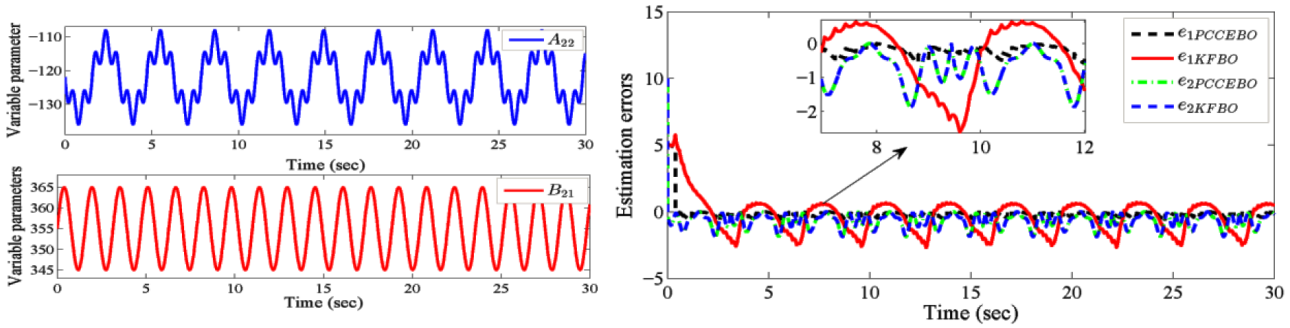

(a) System parameters variation. (b) The estimation errors.

Figure 10. State estimation in case of variable system parameters: a) system parameter variation; b) estimation errors.

For PCCEBO, $P = \begin{bmatrix} 4.9502 & 0.0000 \\ 0.0000 & 4.9502 \end{bmatrix}, Y = \begin{bmatrix} 4.9502 \\ 0.0000 \end{bmatrix}, L = \begin{bmatrix} 1.0000 & 0.0000 \end{bmatrix}^T;$

For KFBO, $Q = \begin{bmatrix} 0.001 & 0 \\ 0 & 0.001 \end{bmatrix}, R = 0.3, P_r = \begin{bmatrix} 0.0712 & 0.0085 \\ 0.0085 & 1.0330 \end{bmatrix}, K = \begin{bmatrix} 0.2374 & 0.0282 \end{bmatrix}^T.$

The corresponding results are illustrated in Figure 11. The simulation results show that the proposed PCCEBO demonstrates a more rapid converge and better performance than the KFBO, and the estimation errors of the PCCEBO are equal to zero after two sampling periods. Thus, the PCCEBO can compensate time delay even if the sampling period is not small. The estimation errors for all examined cases are quantified as shown in Figure 12. The MAE describes the mean absolute error calculated by $\frac{1}{N}\sum_{i=1}^{N}|e_i|$ where $(i = 1, 2, ..., N)$ and RMSE is the root mean square error computed by $\sqrt{\frac{1}{N}\sum_{i}^{N}e_i^2}$. It can be readily noticed that the proposed observer presents better performance and accuracy than the KFBO.

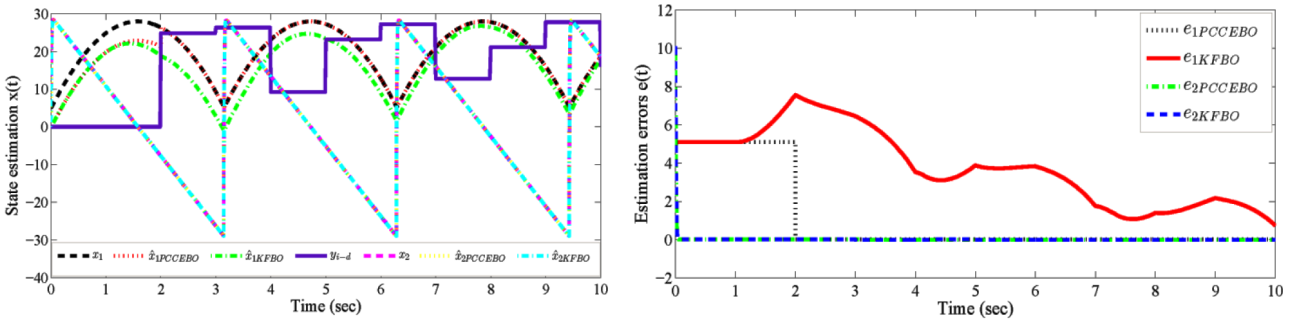

(a) The state and its estimation. (b) The estimation errors.

Figure 11. State estimation for $d = t_e = 1$ s: a) the state and its estimation; b) the estimation errors.

Therefore, from all examined cases, it can be summarized that the proposed PCCEBO presents better performance than the KFBO.

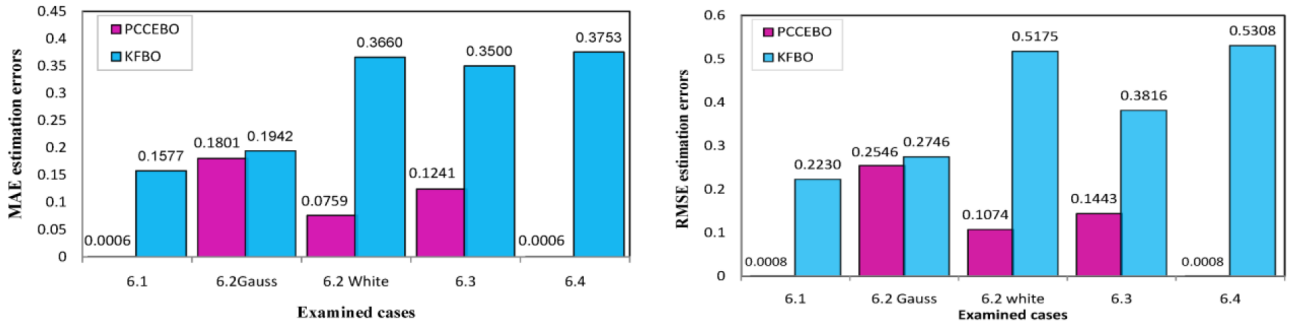

(a) MAE estimation errors. (b) RMSE estimation errors.

Figure 12. The observers' performance and statistical values of the estimation errors: a) MAE estimation errors; b) RMSE estimation errors.

7. Conclusions

In this paper, a piecewise continuous current estimator observer is derived to estimate nondelay continuous states from sampled and delayed signals. The proposed observer is designed to compensate the delay in the feedback channel. Moreover, the stability analysis of the proposed observer is presented. To demonstrate the effectiveness of the proposed approach, comparison with a Kalman filter-based observer has been conducted. Comprehensive numerical simulation results demonstrated that the proposed observer showed better performance than the Kalman filter-based observer.

References

[1] Kelly R, Carelli R, Nasisi O, Kuchen B, Reyes F. Stable visual servoing of camera-in-hand robotic systems. IEEE ASME T Mech 2000; 5: 39-48.

[2] Keshmiri M, Xie WF. Augmented imaged based visual servoing controller for a 6 DOF manipulator using acceleration command. In: IEEE 51st IEEE Conference on Decision and Control; 10–13 December 2012; Maui, HI, USA. New York, NY, USA: IEEE. pp. 556-561.

[3] Korayem MH, Khoshhal K, Ali Akbarpour H. Vision based simulation and experiment for performance tests of robot. Int J Adv Manuf Technol 2005; 25: 1218-31.

[4] Corke PI. High-performance visual closed-loop robot control. PhD, University of Melbourne, Melbourne, Australia, 1994.

[5] Corke PI, Good MC. Dynamic effects in visual closed-loop systems. IEEE T Robotic Autom 1996; 12: 671-83.

[6] Chaumette F, Hutchinson S. Visual servo control. I. Basic approaches. IEEE Robot Autom Mag 2006; 13: 82-90.

[7] Chaumette F, Hutchinson S. Visual servo control. II. Advanced approaches [Tutorial]. IEEE Robot Autom Mag 2007; 14: 109-118.

[8] Monroy C, Kelly R, Arteaga M, Bugarin E. Remote visual servoing of a robot manipulator via Internet2. J Intell Robot Sys T 2007; 49: 171-187.

[9] Chen T, Francis BA. Optimal Sampled-Data Control Systems. 1st ed. London, UK: Springer, 2012.

[10] Åström KJ, Wittenmark B. Computer-Controlled Systems: Theory and Design. 3rd ed. New York, NY, USA: Dover, 2013.

[11] Nilsson J. Real-time control systems with delays. PhD, Lund Institute of Technology, Lund, Sweden 1998.

[12] Ahrens JH, Tan X, Khalil HK. Multirate sampled-data output feedback control with application to smart material actuated systems. IEEE T Autom Control 2009; 11: 2518-2529.

[13] Roberts AP. State estimation when some measurements are delayed. IMA J Math Control I 1986; 3: 299-310.

[14] Hussein MT, Söffker D. State variables estimation of flexible link robot using vision sensor data. In: IFAC 2012 7th Vienna International Conference on Mathematical Modeling; 14–17 February 2012; Vienna, Austria. pp. 193-198.

[15] Wang H, Vasseur C, Koncar V. Piecewise continuous systems used in trajectory tracking of a vision based x-y robot. In: Sobh T, Elleithy K, Mahmood A, Karim MA, editors. Novel Algorithms and Techniques in Telecommunications, Automation and Industrial Electronics. Berlin, Germany: Springer, 2008. pp. 255-260.

[16] Wang HP, Tian Y, Christov N. Piecewise-continuous observers for linear systems with sampled and delayed output. Int J Syst Sci 2014; 1: 1-12.

[17] Chamroo A, Seuret A, Vasseur C, Richard JP, Wang HP. Observing and controlling plants using their delayed and sampled outputs. In: IEEE 2006 Proceedings of the 4th IMACS Multi-Conference on Computational Engineering in Systems Applications; 4–6 October 2006; Beijing, China. New York, NY, USA: IEEE. pp. 851-857.

[18] Koncar V, Vasseur C. Control of linear systems using piecewise continuous systems. IET Control Theory Appl 2003; 150: 565-576.

[19] Šiljak DD, Stipanovic DM. Robust stabilization of nonlinear systems: the LMI approach. Math Probl Eng 2000; 6: 461-49.